

Optimization of Multi-Objective Process Parameters of TIG-MIG Hybrid Welding On EN24 Mild Steel Material Using the Grey-Based Taguchi Method

Fasil Kebede Tesfaye (✉ fasilk@mtu.edu.et)

Mizan-Tepi University <https://orcid.org/0000-0001-8776-6786>

Ayitenew Mogninet Getaneh

Research Article

Keywords: TIG-MIG, Taguchi method, Optimization, Welding Process Parameters, Grey Relational Analysis and Mechanical Properties

Posted Date: June 13th, 2023

DOI: <https://doi.org/10.21203/rs.3.rs-2873251/v1>

License: © ⓘ This work is licensed under a Creative Commons Attribution 4.0 International License.

[Read Full License](#)

Abstract

Metal Industry and Machine Technology Development Enterprise is Ethiopia's leading manufacturing industry, producing a diverse range of industrial machinery and products. The main welding process used to join the products is MIG welding, which has several flaws, including low weld-metal toughness, spatter formation, undercut formation, and finally poor tensile strength and toughness. The company also uses TIG welding, which uses an inert gas to produce less smoke and fumes. While this technology produces precise welds, it is a time-consuming operation with a lower production rate. As a result, a special type of welding process is required that incorporates the properties of both types of welding processes. As a result, the hybrid TIG-MIG welding configuration was proposed. The optimization of process parameters of EN24 mild steel material for TIGMIG hybrid welding is presented in this paper. The test was carried out on a 6 mm EN24 mild steel plate. The butt joint configuration was used. MIG welding current, TIG welding current, MIG welding voltage, TIG welding voltage, and welding gun travel speed were used as process parameters. A single-level L27 orthogonal array is used to optimize process parameters. Tensile and hardness tests are used to evaluate the mechanical properties of the weld joint. The optimum level setting of the test, according to the mean effect plot of GRG, is MIG welding current of 200 A, MIG welding voltage of 15 V, TIG welding current of 200 A, TIG welding voltage of 18 V, and welding gun travel speed of 5 mm/s. The significant process parameters were investigated using ANOVA. MIG welding current and MIG welding voltage were significant factors in the ANOVA, with percentage contributions of 44.19% and 49.20%, respectively. Five confirmation tests were performed, and the results show that the mean grey relational grade of the conformation test was 0.7594, which falls within the 90% confidence interval, indicating that the experiment is reliable. Finally, MIG welding, TIG welding, and TIG-MIG hybrid welding processes were compared, with the results indicating that TIG-MIG hybrid welding has the highest hardness and tensile strength of all. Based on the findings, it is possible to conclude that the company should use the hybrid welding method to improve the weld joint's hardness and tensile strength.

1. Introduction

In any manufacturing industry, welding is widely used to assemble various products. Welding is the process of combining two or more metals that are similar or dissimilar by heating them to an appropriate temperature and then joining them with or without the use of pressure, filler material, and flux. The heat can be provided by an electric arc (in the case of arc welding), gas combustion (in the case of gas welding), electrical resistance (in the case of resistance welding), or black Smith's fire (in the case of resistance welding) (in case of forge welding).

The filler material has a similar composition to the base metal and a lower melting point. The filler rod is used to provide more material, fill the gap between joints, and create a round, oval, or fillet shape. It also serves to compensate for losses that occur during the welding process.

Flux is sometimes used to remove the oxides formed during the process, in the form of fusible slag which floats on the molten metal. This also prevents the re-formation of Oxides by environmental conditions.

Welding of similar metals without filler material is known as autogenesis welding while filler material is called homogeneous welding. On the other hand, the welding of dissimilar metals with filler rods is called heterogeneous welding. The welding phenomenon comes into existence in 1930. Its growth is very fast in the fabrication industry.

It is an alternative method for casting or forging. Welding technology today has a broad and deep scope. It is successfully used in everyday things such as automobiles, planes, ships, home appliances, electronic equipment, bridge construction, building construction, pressure vessels, tanks, rail and road equipment, piping and pipelines, trucks, trailers, and trusses, among others.

TIG and MIG welding are the most popular gas shielded arc welding processes used in many industrial fields. MIG is the welding process that is now used for welding a variety of materials, ferrous and nonferrous. In manual welding operation, the welder must control over a welding variable that affects the weld penetration, weld geometry, and overall weld quality.

Proper changes of weld material like welding current, welding voltage, travel speed, wire electrode size and type shielding gas, weld joint position, and electrode angle will increase the chance of producing welds of satisfactory quality (Jagtap & Raut, 2019).

The working principle of the MIG welding process is the electrode in this process is in the form of a coil and continuously fed towards the work during the process. At the same time, inert gas is passed through electrodes from the same torch. Inert gas usually argon, helium on a suitable mixture of these used to prevent the atmosphere from contacting the molten metal and HAZ when gas is supplied, it gets ionized and the arc is initiated in between electrode and workpiece.

TIG welding consists of features such as less spatters without requiring much post-weld cleaning and better weld bead surfaces than MIG welding with pure Ar. However, TIG welding needs improvement in its efficiency. MIG welding has high efficiency and high rates of metal deposition but it needs some improvement in quality, oxidation of bead surface and spatter to be produced. Because of relatively high productivity and low cost MAG welding is mostly used, but there are some instabilities presented in MAG welding as spatter and weld bead roughness is also existed. Lucas and Tusek suggested that a number of appearance defects typically including undercut and humping weld were easily formed, which limited the further improvement of productivity (Welding et al., 2016).

Combining welding processes have been used since the 1970s. This combination has come to be called hybrid welding, which is a technology that consists of combining different types of welding processes, which operate simultaneously in the same weld puddle, i.e., a new process should result from the combination of two (or more) conventional processes in which the new process offers the effects of which each process individually is incapable (Schneider et al., 2017).

The majority of hybrid welding research focuses on integrating LASER with an electric arc process, such as: LASER associated with the tungsten inert gas (TIG); LASER with metal inert gas (MIG) or metal active

gas (MAG); LASER with plasma arc welding (PAW); and other configurations. Different forms of LASER (CO₂, Nd-YAG, etc.) are employed in various instances. Combinations of electric arc techniques, such as PAW with MIG and TIG with MIG are also employed. According to Kanemaru, the latter has become a low-cost alternative since electric arc welding equipment is less expensive than LASER equipment. (Schneider et al., 2017).

The TIG-MIG hybrid welding process—also known as gas tungsten arc welding (GTAW)/gas metal arc welding (GMAW)—consists of combining the TIG and MIG processes in a single welding process. As shown in Figs. 1.1 and 1.2 this process usually works by using a TIG welding torch running through the work piece, which leads to the melt pool, i.e., at the front of the MIG torch, which heats and forms a keyhole in the source material. Subsequently, the MIG surges and follows the process by filling in the “keyhole” created by the TIG process and adds material because an electric arc and an electrode wire are used. To summarize, the procedure begins with a TIG arc warming and opening a gap in the work piece to allow for deep penetration, followed by a highly efficient MIG deposit of material to complete the operation.

The purpose of hybridizing the TIG and MIG welding process is TIG arc can stabilize the MIG arc by stable hybridization, the process can be a potential method of welding ferrous and non-ferrous metals with low cost and high efficiency. TIG-MIG hybrid welding can double the performance of traditional procedures by increasing weld penetration, providing greater control over the heat-affected zone, and increasing welding speed, all of which result in enhanced productivity. Stable cathode spots also enable high welding speed and quality. The work piece's desired joint characteristic is created by combining the MIG and TIG arcs. (Akinlabi et al., 2019).

2. Materials and Methods

2.1. Workpiece Materials

In this study, the work material used is EN24 mild steel plate as a welding specimen with a butt joint configuration. All specimens were cut off at an equal length of 101.6 mm using a grinder cutter. Figure-3. indicates the solid work model and the fabricated dimension of the specimen.

A chemical composition test was performed in Akaki basic metal industry, and the content of the mild steel material is summarized in table-1, and the physical, mechanical, chemical and thermal properties of EN24 mild steel are summarized in Table-1.

Table-1. Chemical composition of EN24 mild steel

Element Present →	<i>C</i>	<i>Mn</i>	<i>Si</i>	<i>S</i>	<i>P</i>	<i>Cu</i>	<i>Fe</i>	<i>others</i>
Content	0.207	0.393	0.176	0.005	0.076	0.409	98.2	0.448

2.2. Welding Fixture

The workpiece holder (fixture) was made from 50 X 25 X 1.6 Rectangular Hollow Section (RHS) steel with four phases, unipolar, permanent magnet stepper motor. The motor is a standard size NEMA 17 (1.7 in square footprint, 5 mm shaft diameter) 12 V motor with 200 steps per rotation. The stepper motor is controlled by an Arduino IDE 1.8.13 software, and the program for controlling the x-axis movement of the workpiece holder is found in the appendix. In this fixture, the welding guns are mounted on the fixed welding gun holder and the workpiece was fixed on the workpiece holding fixture that travels in x-axis forward and backward. The SolidWorks model of this fixture is shown in Figure-4. A, and the fabricated model of the fixture is shown in Figure-4. B.

2.3. Experimental Work

The target material was selected to be most frequently used in AMIMTDE for manufacturing agricultural and transportation equipment. And a butt joint configuration is selected for the test. All specimens were cut off at equal dimensions of 101.6 mm using a shearing machine and grinder. In addition, after welding the specimen, a mechanical test was prepared according to ASTM E8-04 guidelines. The experimental setup of the welding machine and fixture is shown in Figure-5. A) and Figure-5. B).

2.4 Methods

2.4.1. Determination of Working Limits of Parameters

The ANOVA, or Analysis of Variance, can be used to find statistically significant process characteristics that affect the study's response. The ANOVA, or Analysis of Variance, can be used to find statistically significant process characteristics that affect the study's response.

Different scholars use ANOVA to identify parameters of how much percent contributing to the response of the study. Therefore, the present study, reviewed and determined the most significant process parameters that strongly improved the response of the study. Parameters were collected from a previous similar study of 15 article journals by looking at its average percentage of contribution and after that determined and selected using Pareto principles. The root causes of the selected parameters are also identified by a fishbone diagram. These 15 articles are selected based on the material type selected for this study which mild steel material, the thickness of material (5–8 mm thickness plate), and published date.

3. Results and Discussion

3.1 Introduction

This overall results of the experiments using the application of the Grey relation analysis-based Taguchi method. The experiment was conducted to find the optimum response of hardness and tensile strength of EN 24 mild steel plate. The optimum condition is identified by studying the main effects of parameters. The main effects indicate the common trend of influence of each parameter. The analysis of variance

(ANOVA) is the statistical treatment most commonly applied to the results of the experiments in determining the percent contribution of each parameter against a stated level of confidence.

In this work, the optimization of TIG-MIG hybrid welding parameters on the selected quality characteristics has been investigated through the plots of the main effects based on the obtained data from the experiments. The optimum condition for each of the quality characteristics has been established through S/N data analysis.

3.2. Experimental Result

The experiments were conducted to study the effect of process parameters over the output response characteristics of hardness and tensile strengths, and the five process parameters of MIG welding current, TIG welding current, MIG welding voltage, TIG welding voltage, and welding gun travel speed, and their levels with ultimate tensile strength, and hardness value are listed. Statistical analysis of the data has been carried out using MINITAB 18 software.

3.2.1. Tensile Strength

The maximum stress that a material can sustain while being stretched before failing or breaking is known as tensile strength, often known as ultimate tensile strength or ultimate strength. The test was conducted at room temperature for similar TIG-MIG hybrid welded EN 24 mild steel plate materials. The maximum tensile strength was 540 MPa obtained from a MIG welding current and voltage of 200 A and 15 V with TIG welding current and voltage at 170 A and 24 V, and welding gun travel speed of 10 mm/s. Correspondingly, the minimum tensile strength value of 420 MPa was obtained from a MIG welding current and voltage of 140 A and 20 V with TIG welding current and voltage at 170 A and 18 V, and welding gun travel speed of 7.5 mm/s. The result shows that the tensile strength increases, the MIG and TIG welding current increase and the welding voltage of MIG decrease while TIG welding voltage increases. The tensile strength becomes maximum at a higher welding gun travel speed. The effect of each controlled process parameter on tensile strength is shown in Figure-6.

As shown in Figure-6, the best tensile strength is achieved when TIG welding voltage and TIG welding currents increase and MIG welding voltage and MIG welding current falls.

3.2.2. Hardness

The hardness of the joint was measured three times at the weld joint. The higher hardness value of 72 HR was obtained at a MIG welding current and voltage of 170 A and 15 V respectively, TIG welding current and voltage of 200 A and 18 V, and welding gun traverse speed of 5 mm/s. Similarly, the minimum hardness value of 50 HR was obtained at a MIG welding current and voltage of 140 A and 20 V respectively, TIG welding current and voltage of 170 A and 18 V, and welding gun traverse speed of 7.5 mm/s. As shown in Figure-7. The maximum TIG welding current with a combination of medium level MIG

welding current provides the highest hardness. The MIG welding voltage with a combination of TIG welding voltage and gun travel speed contributes a great influence on the hardness of the joint.

The target material's maximal hardness is imparted by greater MIG and TIG welding currents, as indicated in Figure-7. The amount of weld metal deposited during welding and weld penetration is controlled by the MIG & TIG welding current.

3.2.3 Effect of Welding Parameters on the Joint Quality

The following table shows the effect of welding parameters on the joint strength of the target material

Experiments 1, 3, 18 and 24 have spatter caused by insufficient gas shield & too long arc, and experiment 9, 10, 11, 19, 23 & 25 have porosity on weld zone and is caused by the presence of air bubbles & gas trapped in the weld zone. Experiments 4 & 6 have under-filling defects caused by not being filled with a proper amount of molten metal, and experiment 5 has a slag inclusion defect in the weld zone. The remaining experiments have completely defect-free weld joints. To sum up from all the defect-free experiments the experiment with a MIG welding current of 200 A, MIG welding voltage 15 V, TIG welding current of 170 A, TIG welding voltage of 24 V, and gun travel speed of 10 mm/s produce defect-free and high strength weld joint.

3.3. Grey based Taguchi Analysis

Taguchi technique offers three possibilities for calculating the signal-to-noise (S/N) ratio: greater is better, nominal is best, and smaller is best. The selection of a suitable S/N ratio, on the other hand, necessitates some practical experience, competence, and understanding of the process. The aim of this study is finding the higher hardness and tensile strength that corresponds to a better welding performance. Therefore, larger is better S/N ratio was selected. It was calculated with the following equation (Kasman, 2013)

$$\frac{S}{N} = -10 \log_{10} \frac{1}{n} \sum_{n=1}^i \frac{1}{y^2} \text{ijk}$$

Where n is the number of replications and " y_{ijk} " is the response value of the " i^{th} " performance characteristic in the " j^{th} " experiment at the " k^{th} " trial. The results of the average tensile strength (UTS), Hardness (HRC), and their respective signal to Noise ratio (S/N) are given in Table-2.

Table-2. Experimental results with its S/N ratio

No	UTS [MPa]	Hv [HRC]	S/N _{UTM} [dB]	S/N _{Hv} [dB]
1	481	59.5	53.6491	35.4903
2	507	67	54.1003	36.5215
3	450	54	53.0644	34.6479
4	470	57	53.4421	35.1175
5	420	50	52.4651	33.9794
6	460	55	53.2553	34.8073
7	490	62	53.8038	35.8478
8	480	61	53.6248	35.7066
9	490	63	53.8039	34.3201
10	470	59	53.4420	35.4170
11	430	52	52.6694	34.3201
12	480	59	53.6248	35.4170
13	510	68	54.1514	36.6502
14	500	69	53.9794	36.7770
15	500	65	53.9795	36.2583
16	530	72	54.4855	37.1466
17	505	67	54.0658	36.5216
18	500	65.5	53.9794	36.3249
19	520	70	54.3201	36.9021
20	490	64	53.8039	36.1235
21	450	58.5	53.0643	35.3432
22	430	66	52.6694	36.308
23	490	63.5	53.8039	36.0555
24	540	72	54.6479	37.1466
25	510	68	54.1514	36.6502
26	500	65	53.9794	36.2583
27	480	62	53.6249	35.7778

3.4. Grey Relation Analyses

Taguchi methodology is primarily used to reduce the number of tests by using orthogonal arrays, which are specially created tables. In this work L27 array is used to conduct the experiments. This consists of three parameters and three levels. Mostly Taguchi method is used for the optimization of a single parameter (i.e. Mono-objective optimization). Optimization based on multiple factors can be done easily and successfully by combining Taguchi with grey relational analysis. The grey relational analysis entails calculating a grey relational coefficient for each parameter, then taking the average of all grey relational coefficients to determine the grey relational grade, which is then utilized as the response for the L27 orthogonal array. (Sampath et al., 2016)

Grey relational analysis (GRA) is an efficient tool for optimizing multi-response conditions. This analysis method is used for solving the sophisticated interconnection among the multi objective responses. GRA has seven steps for optimizing multiple responses. (Sahu & Pal, 2015) In this study, followed the following steps:

3.5. Principal Component Analysis

Principal component analysis (PCA) is a dimensionality reduction method that is commonly used to reduce the dimensionality of large data sets by reducing a large collection of variables into a smaller set that still contains the majority of the information in the large set. To reduce the response correlation, PCA was utilized. This matrix consists of Eigen values, Eigen vectors, and quality characteristics contributions. The elements of the array for multiple performance characteristics listed in Table-3, - Table-5, represent the grey relational coefficient matrix and determine the corresponding Eigen value.

Table-3. Eigen values and explained variation

Principal component	Eigen Value	Eigen Value Explained Variation (%)
UTS	1.2825	64.13
Hv	0.7175	35.87

The principal component with the highest Eigen values is chosen to replace the original responses for further analysis. In this case, the highest Eigen values were obtained in the UTS first principal component. Then, the contribution of each individual quality characteristic for the first principal components is shown in Table-4.

Table-4. Eigenvectors for principal component

Quality characteristics	Eigen Vector	
	1st Principal	2nd Principal
UTS	0.707	-0.707
Hv	0.707	0.707

Table-5. Quality characteristic contribution

UTS	0.499
Hv	0.499

Therefore, the grey relational coefficient values is taken as $\xi = 0.5$.

Table-6. Data normalization and deviation sequence

Step:1 Data Normalized			Step:2 Deviation Sequence	
No	UTS	Hv	UTS	Hv
1	0.5083	0.3438	0.4917	0.6563
2	0.7250	0.8125	0.2750	0.1875
3	0.2500	0.0000	0.7500	1.0000
4	0.4167	0.1875	0.5833	0.8125
5	0.0000	-0.1250	1.0000	1.2500
6	0.3333	0.0625	0.6667	0.9375
7	0.5833	0.5000	0.4167	0.5000
8	0.5417	0.4375	0.4583	0.5625
9	0.6250	0.5625	0.3750	0.4375
10	0.4583	0.3125	0.5417	0.6875
11	0.0833	-0.1250	0.9167	1.1250
12	0.5000	0.3125	0.5000	0.6875
13	0.7500	0.8750	0.2500	0.1250
14	0.6917	0.9375	0.3083	0.0625
15	0.6667	0.6875	0.3333	0.3125
16	0.9167	1.1250	0.0833	-1250
17	0.7083	0.8125	0.2917	0.1875
18	0.6750	0.7188	0.3250	0.2813
19	0.8333	1.0000	0.1667	0.0000
20	0.6500	0.6250	0.3500	0.3750
21	0.2917	0.2813	0.7083	0.7188
22	0.6417	0.7500	0.3583	0.2500
23	0.6083	0.5938	0.3917	0.4063
24	1.0000	1.1250	0.0000	0.1250
25	0.7500	0.8750	0.2500	0.1250
26	0.6667	0.6875	0.3333	0.3125
27	0.5583	0.4688	0.4417	0.5313

3.6. Calculation of Grey Relational Coefficient and Grades

The average of the grey relational coefficient is usually considered as the grey relational grade after obtaining the grey relational coefficient. The level of correlation between the reference sequence and the comparability sequence is shown by the grey relational grade. The grey relational grade is a weighted average of multi-objective grey relational coefficients. (Kumar, 2013). It is determined by the following equation.

Table-7. Grey relation coefficient, Grey relation Grade & its rank

Grey Relational Coefficient			Grey Relational Grade & Its Rank	
No	UTS	Hv	GRG	Rank
1	0.5042	0.4324	0.4683	19
2	0.6452	0.7273	0.6862	7
3	0.4000	0.3333	0.3667	25
4	0.4615	0.3810	0.4212	22
5	0.3333	0.2857	0.3095	27
6	0.4286	0.3478	0.3882	24
7	0.5455	0.5000	0.5227	16
8	0.5217	0.4706	0.4962	18
9	0.5714	0.5333	0.5524	15
10	0.4800	0.4211	0.4505	21
11	0.3529	0.3077	0.3303	26
12	0.5000	0.4211	0.4605	20
13	0.6667	0.8000	0.7333	6
14	0.6186	0.8889	0.7537	4
15	0.6000	0.6154	0.6077	12
16	0.8571	1.3333	1.0952	2
17	0.6316	0.7273	0.6794	8
18	0.6061	0.6400	0.6230	10
19	0.7500	1.0000	0.8750	3
20	0.5880	0.5714	0.5798	13
21	0.4138	0.4103	0.4120	23
22	0.5825	0.6667	0.6246	9
23	0.5607	0.5517	0.5562	14
24	1.0000	1.3333	1.1667	1
25	0.6667	0.8000	0.7333	6
26	0.6000	0.6154	0.6077	12
27	0.5310	0.4848	0.5079	17

Grey Relational Coefficient		Grey Relational Grade & Its Rank		
No	UTS	Hv	GRG	Rank
Average = 0.5928				

3.7. Determination of the Optimal Level of Each Parameter

The main effect analysis of GRG is adopted to figure out the response table for grey relational analysis. The average of each response characteristic for each level of each component is shown in Table-8. The highest minus the lowest average of each factor is shown as the delta static. The ranks of optimum parameters are assigned by Minitab based on delta values; for example, rank 1 is the highest delta value, rank 2 is the second delta value, and so on. The mean response refers to the average value of the performance characteristic for each parameter at different levels, and these ranks show the relative relevance of each element to the response.

Table-8. Main effect of GRG

Levels	Parameters				
	MIG Welding Current [A]	TIG Welding Current [B]	MIG Welding Voltage [C]	TIG Welding Voltage [D]	Gun Travel Speed [E]
1	0.4678	0.5143	0.6962*	0.6072*	0.6582*
2	0.6371	0.6179	0.4676	0.55981	0.5554
3	0.6736	0.6469*	0.6147	0.5733	0.5650
Delta	0.2058*	0.1326	0.2286	0.0339	0.1028
Rank	2	3	1	5	4

Considering the highest GRG value for each parameter in the above table and the marked points in Fig. 4.8 the optimal parameter setting are MIG welding current (A3) 200 A, MIG welding voltage (C1) of 15 V, TIG welding current (B3) of 200 A, TIG welding voltage (D1) of 12 V, and welding gun travel speed (E1) of 5 mm/s are an optimal parameter combination for the multiple performance characteristics. Based on the results presented in Table-11, MIG welding voltage has the largest effect on the hardness and tensile strength of the welded joint Figure-11, shows the GRG interaction plot between the controlled factors, as well as the relationship between the five controlled factors, with lines that cross each other indicating that they have more interaction than those lines that are parallel to each other. And based on the interaction plot almost every process parameter with every single level cross each other indicating that they relate to each other, and the effect of one parameter affects another parameter.

3.8. Performing Analysis of Variance

The analysis of variance (ANOVA) is a statistical method that divides a data set's observed aggregate variability into two parts: systematic components and random factors. The Analysis of Variance (ANOVA) was done to indicate significant parameters. The ANOVA results were used in finding out the effect of the factors on the grey relational grade. At a 90% confidence level if the ANOVA table F-value is greater than the F-value reading from a standard table, then the factor or parameter is considered as a significant factor.

To establish which parameter has a substantial impact on performance attributes, statistical software with an ANOVA analytical tool is utilized. The ANOVA findings for the grey relationship grades are shown in Table-9.

Table-9. ANOVA results for a grey relational grade (GRG)

No	Source	Unit	DF	Adj. SS	Adj. MS	F-Value	P-Value	Contribution	Remark
1	MIG W.C [A]	A	2	0.2169	0.108436	3.35	0.061	44.1953	S
2	TIG W.C [B]	V	2	0.0869	0.043455	1.34	0.289	——	IS
3	MIG W.V [C]	A	2	0.2415	0.120772	3.73	0.047	49.2085	S
4	TIG W.V [D]	V	2	0.0055	0.002766	0.09	0.919	——	IS
5	G.T.S [E]	Mm/s	2	0.0581	0.029031	0.9	0.428	——	IS
6	Error		16	0.5186	0.03241	——	——	6.5962	——
Total			26	0.5028				100%	
F_{0.1(2,16)} = 2.67									

Where: - MIG W.C: MIG welding current, MIG. W.V: MIG welding voltage, TIG W.C: TIG welding current, TIG W.V: TIG welding voltage, G.T.S: welding gun travel speed, S: significant And IS: insignificant.

4. Confirmation Experiment

The confirmation test was conducted on five samples at optimal setting conditions of TIGMIG hybrid welding parameters: A3 (MIG welding current of 200 A), B3 (TIG welding current of 200 A), C1 (MIG welding voltage of 15 V), D1 (TIG welding voltage of 12 V), and E1 (welding gun travel speed of 5 mm/min). A 90% confidence interval for the predicted mean of grey relational grade ("μ" GRG) on a confirmation test was calculated using the following equations

$$\mu_{A3B3C1D1E1} = IGRG + (A3 - IGRG) + (C1 - IGRG) \text{ ————— (1)}$$

Where IGRG is the overall mean of grey relational grade = 0.5724. A3 and C1 are the mean values of grey relational grade with parameters at optimum levels. They are the two significant process parameters.

$$\mu_{A3B3C1D1E1} = 0.5929 + (0.6736 - 0.5929) + (0.6962 - 0.5929) = 0.7769$$

The predicted mean of the grey relational grade in the confirmation test is estimated by the following equation: confidence interval for the predicted mean on a confirmation run is calculated using the below equation

$$CI = \mu \pm \sqrt{F_{\alpha; (1 : fe)} * Ve \left(\frac{1}{neff} + \frac{1}{r} \right)} \quad (2)$$

Where $F_{\alpha; (1, fe)} = F_{0.1; (1, 16)} = 3.05$ (F-Table in the Appendices C)

$\alpha = \text{Risk} = 0.1$

$fe = \text{Error DOF} = 16$ (F-Table in the Appendices C)

$Ve = \text{Error adjusted mean square (ANOVA table in Appendices J)} = 0.03241$

$neff = \text{Effective number of replications}$

$R = \text{Number of replications for confirmation experiment} = 5$

Also the effective number of replications ($neff$) is calculated by:

$$neff = Tn / (1 + TS) = 27 / 1 + 4 = 5.4$$

Where $neff$ is expressed in mathematical

$Tn = \text{Total number of experiments} = 27$

$Ts = \text{the sum of the total degree of freedom of significant factors} = 4.$

Therefore, the calculated CI is

$$CI = \mu \pm \sqrt{F_{\alpha; (1 : fe)} * Ve \left(\frac{1}{neff} + \frac{1}{r} \right)}$$

$$CI = 0.7769 \pm \sqrt{3.05 * 0.03241 \left(\frac{1}{5.4} + \frac{1}{5} \right)}$$

$$= 0.7769 \pm 0.1951$$

The 90% confidence interval of the predicted optimal grey relational grade is:

$$(\mu - CI) < \mu < (\mu + CI)$$

$$= 0.7769 - 0.1951 < \mu < 0.7769 + 0.1951$$

$$= 0.5818 < \mu < 0.9720$$

Based on the 90% confidence level the mean of grey relational grade (“ μ ” GRG) on a confirmation test was expected to lie between 0.5818 and 0.972.

The effectiveness of the optimal condition can be ensured if the predicted and observed GRG values of the different performance parameters are close to each other. To put the theory to the test, the predicted outcomes were confirmed five times under optimum conditions. The grey relational grade for the conformation test experiment is 0.75948, which is in the range of the 90% confidence level.

The confirmation test achieved hardness and tensile strength of 71.2 HR and 539.4 MPa respectively. Hence, the results of the confirmatory experiment tests show that the experiment is safest. Table-10, indicates the grey relational grade value for both the conformation test and for the predicted value.

Table-10. Result of the confirmation tests

	Optimal Parameters	
	Predicted	Experimental
Setting levels	A ₁ B ₁ C ₁ D ₁ E ₁	A ₁ B ₁ C ₁ D ₁ E ₁
Tensile Strength		529.5
Hardness		71.16
Grey Relational Grade	0.7769	0.75948

5. Conclusions

In this study, a combination of grey relational analysis and the Taguchi method was implemented to find the optimal conditions for TIG-MIG hybrid welding parameters to analyze the effect of combined factors on the mechanical strength such as UTS and Hv. Based on the single level L27 orthogonal array, an experimental plan was conducted and the data taken from the experiments were analyzed using GRA. The following conclusions were made.

- In this research several research papers were reviewed to select the basic process parameters and their respective levels and based on the Pareto chart MIG welding current, TIG welding current, MIG welding voltage, TIG welding voltage and gun travel speed are the most basic process parameters out of nine process parameters analyzed and their levels are selected based on machine working range and the frequency the scholars use them, and then based on the selected levels and process parameters a single level L27 orthogonal array was found to be the right orthogonal array for this experiment.

- The highest hardness of 72 HR and tensile strength of 540 MPa was achieved at a parameter setting of MIG welding current of 200 A, TIG welding current of 170 A, MIG welding voltage of 15 V, TIG welding voltage of 24 V, and welding gun travel speed of 10 mm/s. Similarly, the lowest hardness and tensile strength of 50 HR and 420 MPa respectively, were observed at a MIG welding current of 140 A, TIG welding current of 170 A, MIG welding voltage of 20 V, TIG welding voltage of 18 V, and welding gun travel speed of 7.5 mm/s.
- The optimum level setting was determined using the mean grey relational grade value, and it is as follows: MIG welding current of 200 A, TIG welding current of 200 A, MIG welding voltage of 15 V, TIG welding voltage of 12 V, and gun travel speed of 5 mm/s.
- Based on ANOVA results, the MIG welding current, and MIG welding voltage are significant parameters at a 90% confidence interval. The contribution of MIG welding current and MIG welding voltage for hardness and tensile strength was 44.19% and 49.20% respectively and has an error of 6.59%. According to the findings of the confirmation test, the mean gray relational grade of the conformation test was 0.75948, which is between the 90 percent confidence interval of 0.5818 and 0.9720, indicating that the experiment is safe.
- Due to lack of SEM, a visual inspection for the defect was conducted for all 27 experiments and it was found out that out of 27 experiments 12 experiments has defects, and the most commonly occurring defects are: spatter, under filling, porosity, and slag inclusion. To sum up, from the remaining 15 defects free experiment the experiment with a MIG welding current of 200 A, MIG welding voltage of 15 V, TIG welding current of 170 A, TIG welding voltage of 24 V and welding gun travel speed of 10 mm/s has the best tensile strength and hardness.
- The experiment and ANOVA result indicate that the MIG welding current and MIG welding voltage are significant influences on the formation of defects, the hardness and subsequently tensile strength of TIG-MIG hybrid welded EN24 mild steel material.
- From the experiment, the hardness and tensile strength of the MIG welding system, TIG welding system, and TIG-MIG hybrid welding system are compared and based on the comparison the TIG-MIG hybrid welding process has the highest tensile strength with a value of 539.4 MPa and hardness of 71.66 HR. next to hybrid welding system the TIG welding system has second-best tensile strength with a value of 439.33 MPa, and hardness of 70.33 HR, and finally comes the MIG welding process with tensile and hardness strength of 429.33 and 61 respectively.
- The overall results of the study showed that the TIG-MIG hybrid welding process imparts a better hardness and tensile strength on the weld joint, and the comparison between the old working process of the company (MIG welding process) and the new proposed welding process (TIG-MIG hybrid welding process) show that there is an increase in the value of hardness and tensile strength. The hardness and tensile strength of weld joint increases by 10.66 HR and 100 MPa when welded by new proposed welding processes.
- Based on the experimental result obtained the new proposed welding process is suitable for welding a thick plate with thickness ranging from 6 mm – 10 mm, and also the process has less spark which gives the welder a more clear visual of the welding zone. Based on the experiment result the new

proposed TIG-MIG hybrid welding process produces a much better weld joint in terms of tensile strength, hardness and defect, so the AMIMTDE must adopt this process.

- To summarize, different process parameters impart different results and a combination of controlled and uncontrolled parameters provides significant results on the appearance, and mechanical property of weld joint. TIG welding current, MIG welding current, TIG welding voltage. MIG welding voltage and welding gun travel speed parameters were observed and based on the ANOVA result out of five controlled parameters welding current and MIG welding voltage influence the hardness and tensile strength of EN 24 mild steel material. A comparison was made between the three welding processes and the result shows that the TIG-MIG hybrid welding process has superlative mechanical property compared to the MIG, and TIG welding process.

Declarations

Funding Information: There is no outside funding for this research work.

Competing Interests: The authors declare that they have no conflicts of interest. No conflicts of interest exist between the authors and the publication of this research paper, they claim.

Authors' Contribution: GT conducted a review, experimental result and data and analyzed theoretical data. The authors, Fasil Kebede Tesfaye and Ayitenew Mogninet Getaneh, provided comments and checked the paper's quality; as a result.

Acknowledgments

The authors are appreciative that my family provided financial support for this research. Additionally, I would like to thank the Mizan-Tepi University Mechanical Department for allowing me to use their welding equipment.

References

1. Akinlabi, S. A., Mashinini, M. P., Abima, C. S., Fatoba, O. S., & Akinlabi, E. T. (2019). TIG & MIG hybrid welded steel joint: A review. *Proceedings of the International Conference on Industrial Engineering and Operations Management*, 801–811.
2. Angaria, S., Rao, P. S., & Dhimi, S. S. (2017). Optimization of MIG Welding Process Parameters: A Review. *Research Journal of Engineering and Technology*, 8(3), and 273.
3. Chauhan, V., & Jadoun, R. S. (2015). Parametric Optimization of Mig Welding for Stainless Steel (Ss-304) and Low Carbon Steel Using Taguchi Design Method. *International Journal of Recent Scientific Research*, 6(2), 2662–2666.
4. Cheng, Z., Huang, J., Ye, Z., Chen, Y., Yang, J., & Chen, S. (2019). Microstructures and mechanical properties of copper-stainless steel butt-welded joints by MIG-TIG double sided arc welding. *Journal of Materials Processing Technology*, 265, 87–98.

5. Ding, M., Liu, S. S., Zheng, Y., Wang, Y. C., Li, H., Xing, W. Q., Yu, X. Y., & Dong, P. (2015). TIG-MIG hybrid welding of ferritic stainless steels and magnesium alloys with Cu interlayer of different thickness. *Materials and Design*, *88*, 375–383.
6. Fasil Kebede Tesfaye. (2023) Parameter Optimization of Gas Metal Arc Welding Process for Welding Dissimilar Steels. *American Journal of Mechanical and Industrial Engineering*. Vol. 8, No. 1, pp. 1-6. doi: 10.11648/j.ajmie.20230801.11
7. Huang, J., Chen, H., He, J., Yu, S., Pan, W., & Fan, D. (2019). Narrow gap applications of swing TIG-MIG hybrid welding's. *Journal of Materials Processing Technology*, *271*(April), 609–614.
8. Jagtap, M. D., & Raut, N. (2019). Parametric optimization of MIG welding on IS 1079 HR 2 by Taguchi method. *Lecture Notes in Mechanical Engineering*, 81–88.
9. Jeyaprakash, N., Haile, A., & Arunprasath, M. (2015). The Parameters and Equipment's Used in TIG Welding: A Review. *The International Journal of Engineering and Science*, 2319–1813.
10. Kanemaru, S., Sasaki, T., Sato, T., Era, T., & Tanaka, M. (2015a). Study for the mechanism of TIG-MIG hybrid welding process. *Welding in the World*, *59*(2), 261–268.
11. Kanemaru, S., Sasaki, T., Sato, T., Era, T., & Tanaka, M. (2015b). Study for the mechanism of TIG-MIG hybrid welding process. *Welding in the World*, *59*(2), 261–268.
12. Kanemaru, S., Sasaki, T., Sato, T., Mishima, H., Tashiro, S., & Tanaka, M. (2014). Study for TIG-MIG hybrid welding process. *Welding in the World*, *58*(1), 11–18.
13. Kebede F (2021) Carbon-Carbon Composite Application Areas and Limitations. *J Ergonomics*.11: 283.
14. Koli, Y., Yuvaraj, N., Vipin, & Aravindan, S. (2019). Investigations on weld bead geometry and microstructure in CMT, MIG pulse synergic and MIG welding of AA6061-T6. *Materials Research Express*, *6*(12).
15. Kumar, S., & Scholar, M. T. (2019). Comparative Study of Different Welding Processes and Optimization Methods: A Review. *International Journal for Research in Engineering Application & Management (IJREAM)*, *05*(02), 2.
16. [16] Li, L., Orme, K., & Yu, W. (2005). Effect of joint design on mechanical properties of AL7075 weldment. *Journal of Materials Engineering and Performance*, *14*(3), 322– 326.
17. Liu, L., & Zhou, Y. (2019). Mechanism analysis of free formation of backing weld by the pulsed MAG-TIG double arc tandem welding. *China Welding (English Edition)*, *28*(4), 8–15.
18. Lu, D., Cui, L., Chen, H., Chang, Y., Peng, Z., & He, D. (2018). Laser-MIG hybrid keyhole welded 6mm steel/aluminum butt joints. *Materials Science Forum*, *944 MSF*, 581–592.
19. Meng, X., Qin, G., Zhang, Y., Fu, B., & Zou, Z. (2014). High speed TIG-MAG hybrid arc welding of mild steel plate. *Journal of Materials Processing Technology*, *214*(11), 2417–2424.
20. Nair, S. S., & Author, C. (2013). Experimental Investigation of Multipass Tig Welding Using Response Surface Methodology. *Int. J. Mech. Eng. & Rob. Res*, *2*(3).

21. Ogundimu, E. O., Akinlabi, E. T., & Erinosh, M. F. (2018). Study on microstructure and mechanical properties of 304 stainless steel joints by TIG-MIG hybrid welding. *Surface Review and Letters*, 25(1).
22. Pipavat, K. B., Pandya, D., & Patel, V. (2014). Optimization of MIG welding Process Parameter using Taguchi Techniques. *International Journal of Advance Engineering and Research Development*, 1(05).
23. Sahasrabudhe, O. S., & Raut, D. N. (2018). Analytic framework on parameter ranking for hybrid TIG MAG arc welding of mild steel. In *Journal of Advanced Research* (Vol. 12). Cairo University.
24. Samir Khan, M., Kumar, V., Mandal, P., & Chandra Mondal, S. (2018). Experimental Investigation of Combined TIG-MIG Welding for 304 Stainless Steel Plates. *IOP Conference Series: Materials Science and Engineering*, 377(1).
25. Sampath, K. S., Rajasekaran, T., Arun, K. S., & Amrishraj, D. (2016). Optimization of process parameters during Friction Stir Welding of dissimilar aluminum alloys using Grey relational analysis. *Journal of Chemical and Pharmaceutical Sciences*, 9(3), 1647– 1653.
26. Satyaduttsinh P. Chavda, Jayesh V.Desai, T. M. P. (2014). A Review on Optimization of MIG Welding Parameters using Taguchi's DOE Method. *International Journal of Engineering and Management Research*, 4(1), 2250–2758.
27. Schneider, C., Lisboa, C., Silva, R., & Lermen, R. (2017). Optimizing the Parameters of TIGMIG/ MAG Hybrid Welding on the Geometry of Bead Welding Using the Taguchi Method. *Journal of Manufacturing and Materials Processing*, 1(2), 14.
28. Shao, Q., Tan, F., Li, K., Yoshino, T., & Guo, G. (2021). Multi-Objective Optimization of MIG Welding and Preheat Parameters for 6061-T6 Al Alloy T-Joints Using Artificial Neural Networks Based on FEM. *Coatings*, 11(8), 998.
29. Somani, C. A., & Lalwani, D. I. (2019). Experimental investigation of TIG-MIG hybrid welding process on austenitic stainless steel. *Materials Today: Proceedings*, 18, 4826– 4834.
30. Vijayan, D., & Seshagiri Rao, V. (2018). Process Parameter Optimization in TIG Welding of AISI 4340 Low Alloy Steel Welds by Genetic Algorithm. *IOP Conference Series: Materials Science and Engineering*, 390(1).
31. Welding, M. A. G., Karwande, A. S., & Chavan, R. V. (2016). A Review on Experimental Investigation of SS 316 by using TIG-. 6(5), 4792–4794.
32. Zong, R., Chen, J., & Wu, C. (2019). A comparison of TIG-MIG hybrid welding with conventional MIG welding in the behaviors of arc, droplet and weld pool. *Journal of Materials Processing Technology*, 270(October 2018), 345–355.
33. Fasil Kebede Tesfaye and Ayitenew Mogninet Getaneh [2023], Gas Metal Arc Welding Process Variables Enhancement for Welding Significantly different Steels, *Journal of Oil and Gas Research Reviews*. 3(1), 15-20.

Figures

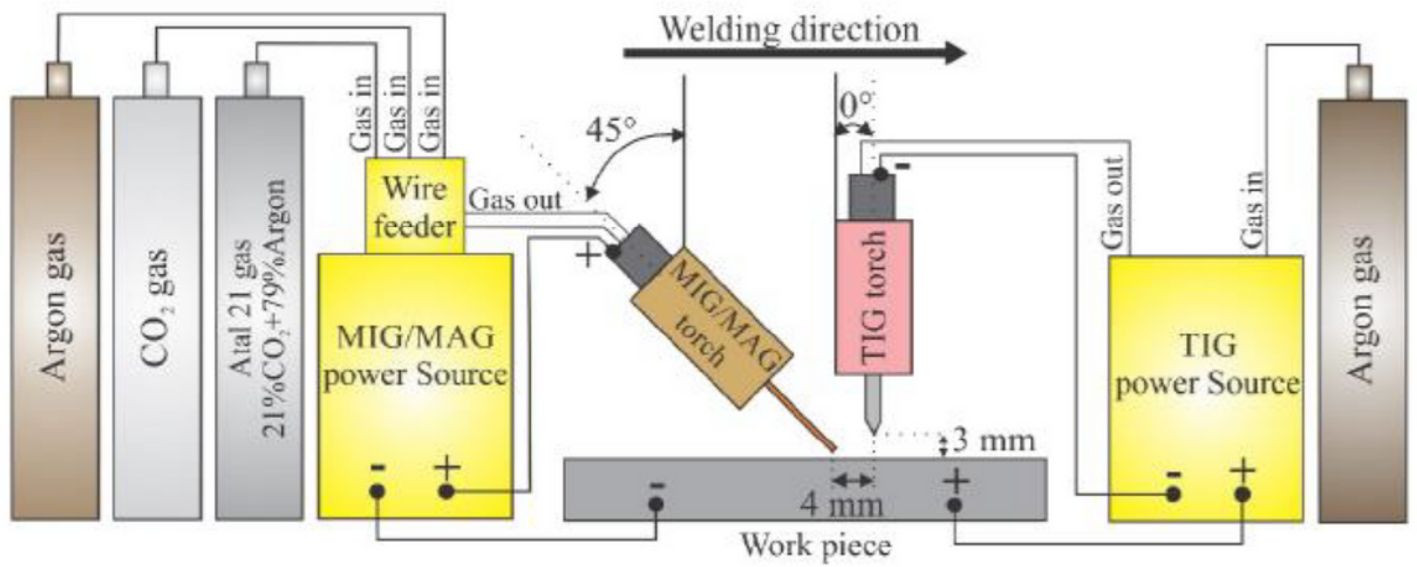


Figure 1

working configuration of TIG-MIG hybrid welding (Schneider et al., 2017)

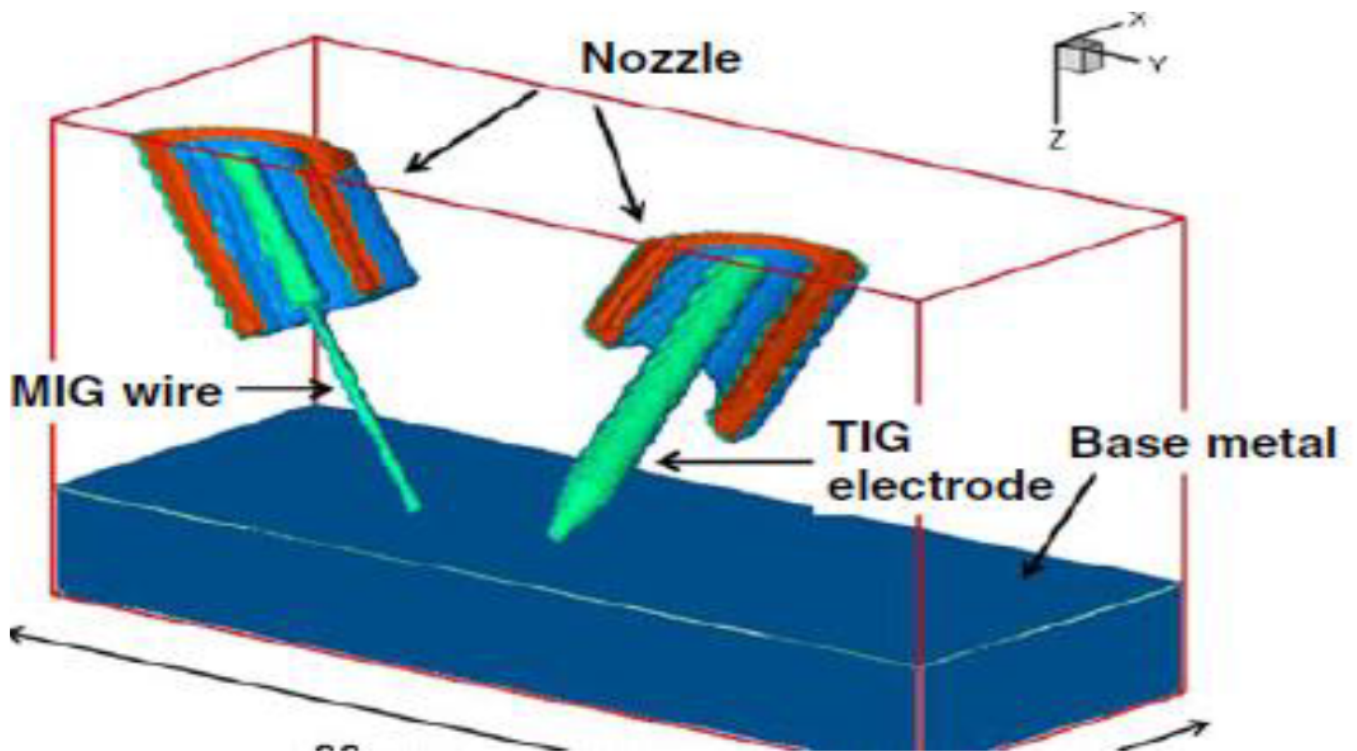


Figure 2

Schematic diagram of TIG-MIG hybrid welding (Kanemaru et al., 2014)

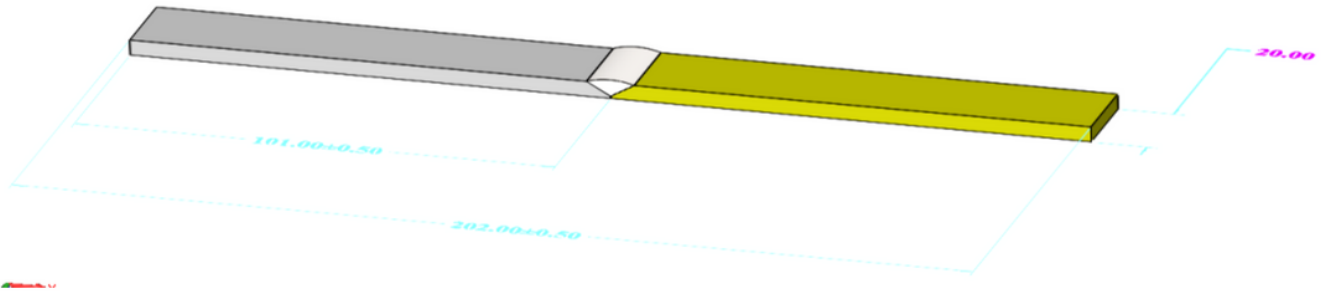
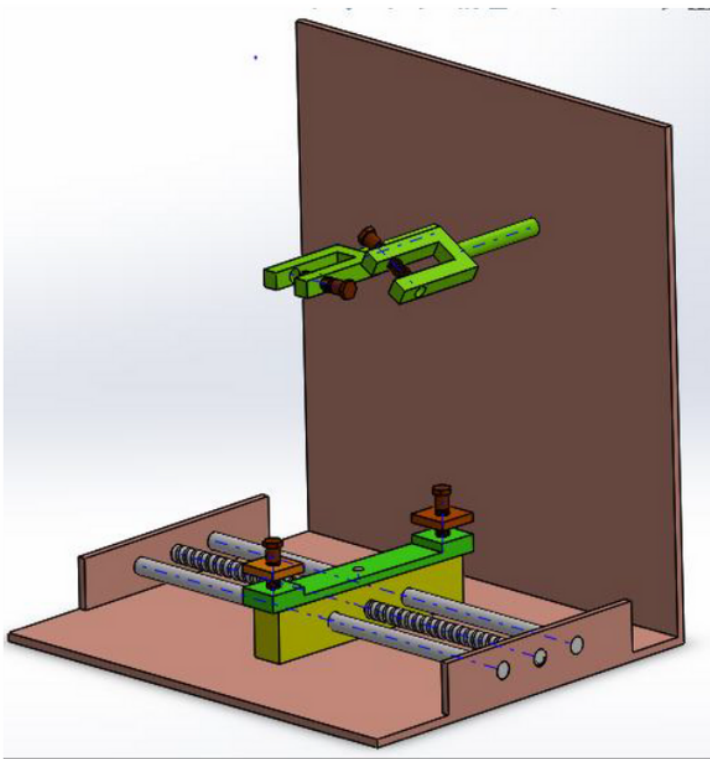
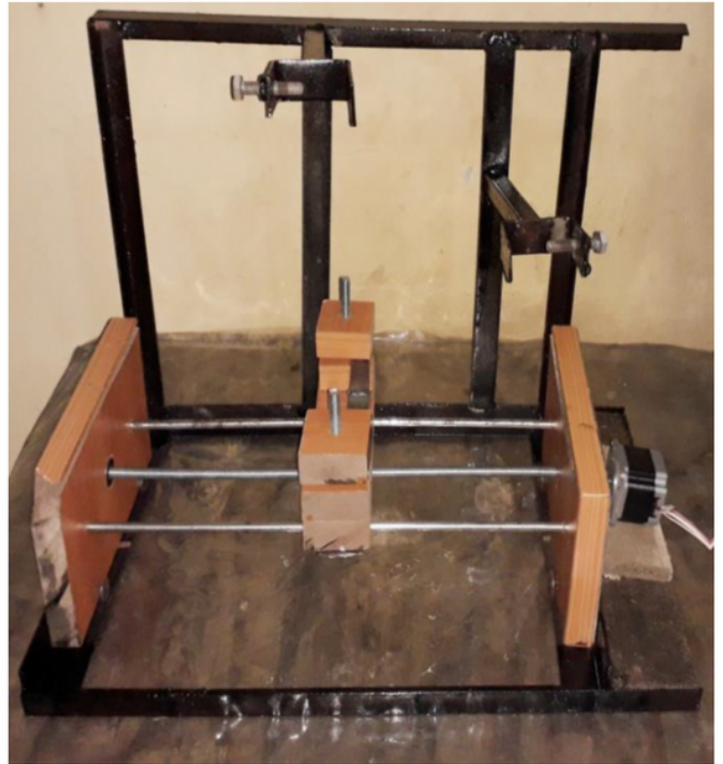


Figure 3

(a) Solid work model of Specimen dimension



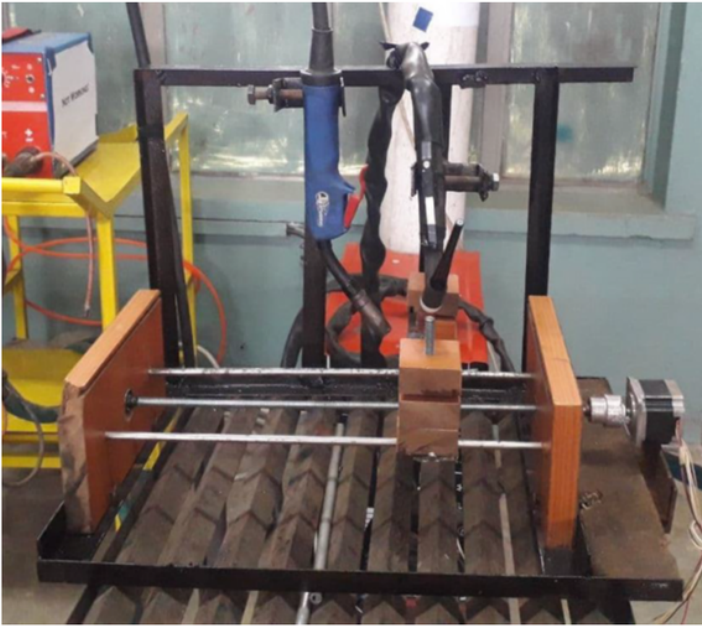
A)



B)

Figure 4

(A) Solid work modeling of the fixture, & (B) Fabricated model of fixture



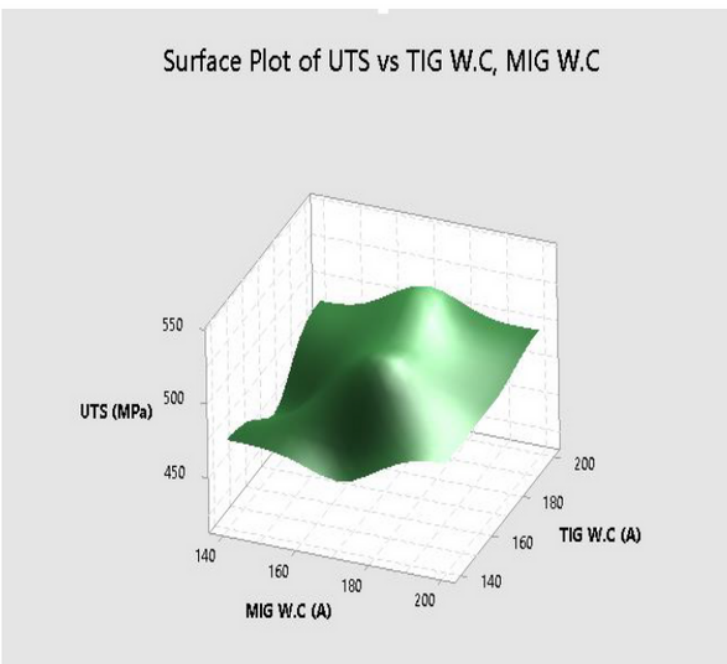
a)



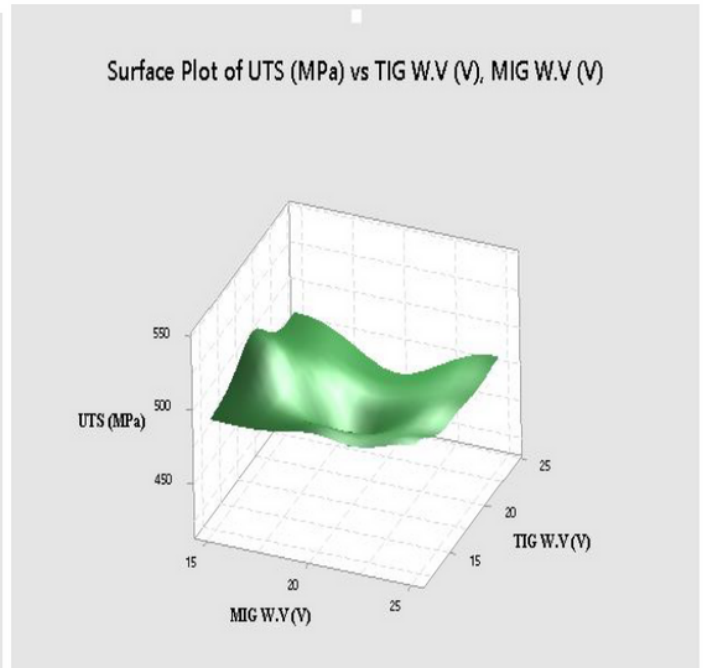
b)

Figure 5

A) Front side and Figure-5. B) Left side experimental Setup



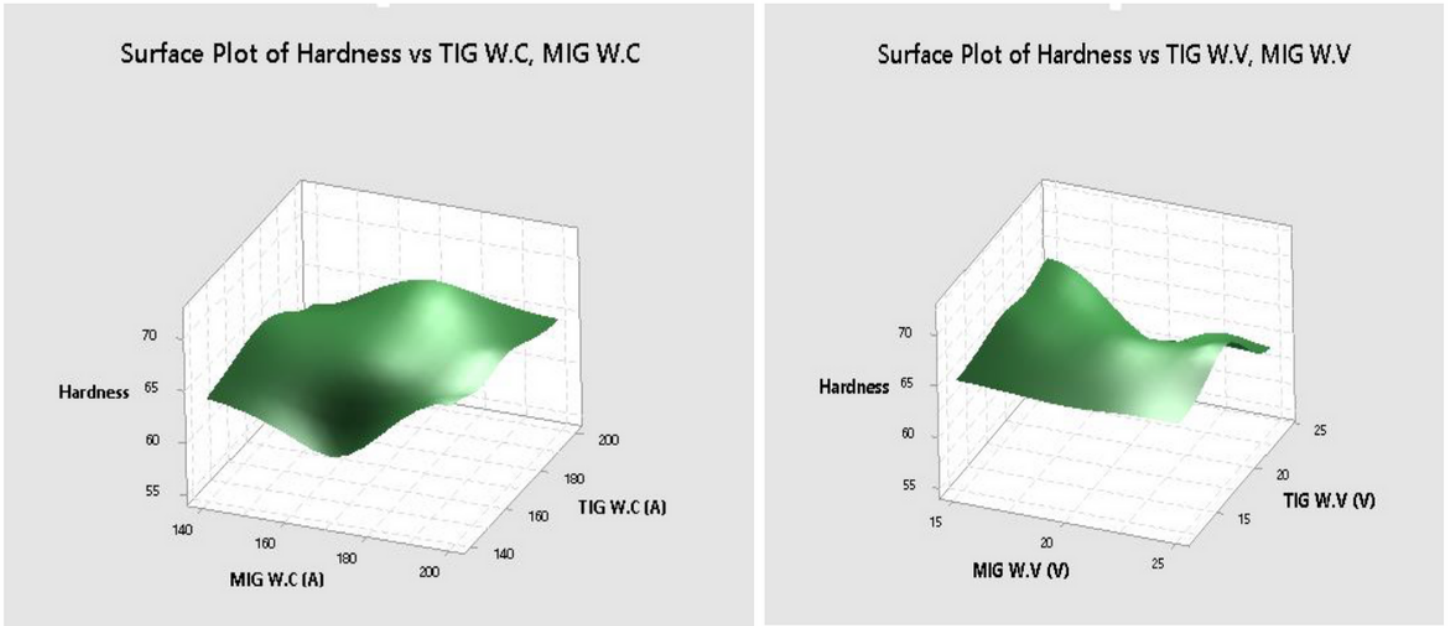
a)



b)

Figure 6

a) Relationship between UTS, MIG and TIG welding current. b) Relationship between UTS, MIG, and TIG welding voltage



A)

B)

Figure 7

A) Relationship b/n Hardness MIG and TIG welding current. B) Relationship b/n Hardness, MIG and TIG welding voltage

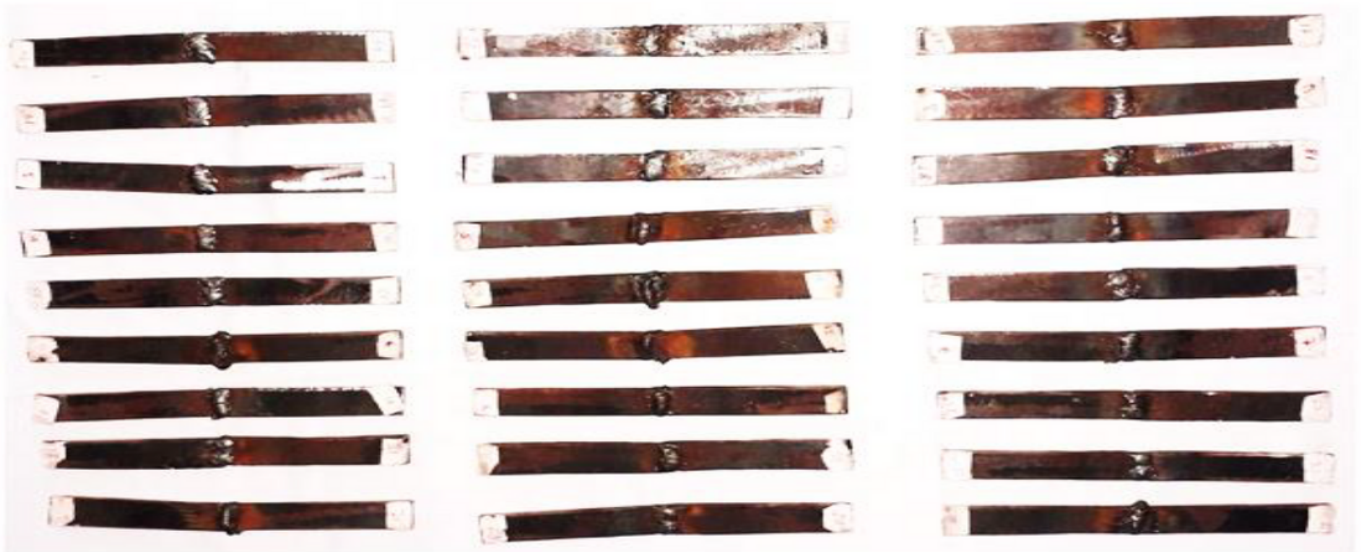


Figure 8

Hardness test specimens

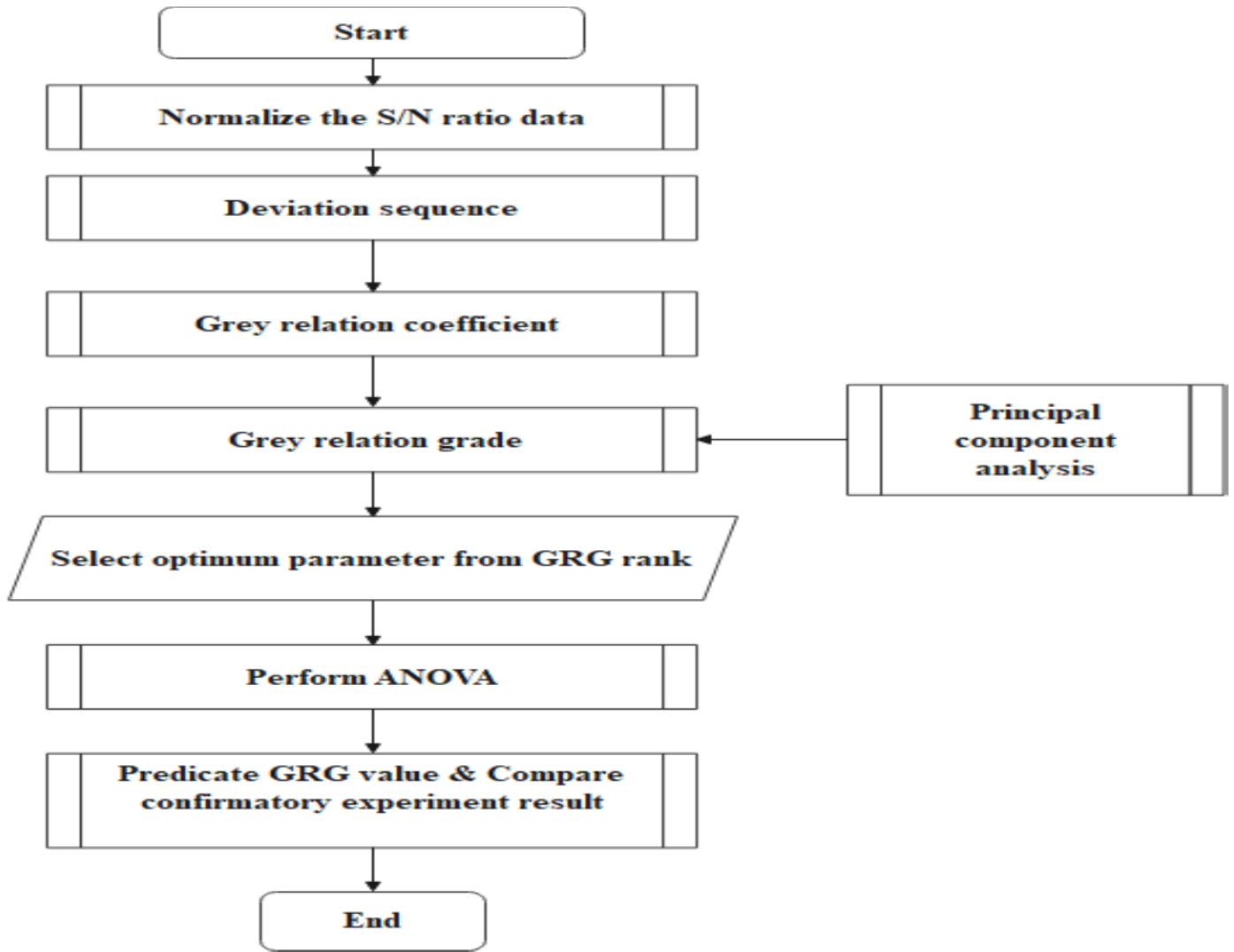


Figure 9

Steps of Grey relational analysis to optimize multiple responses

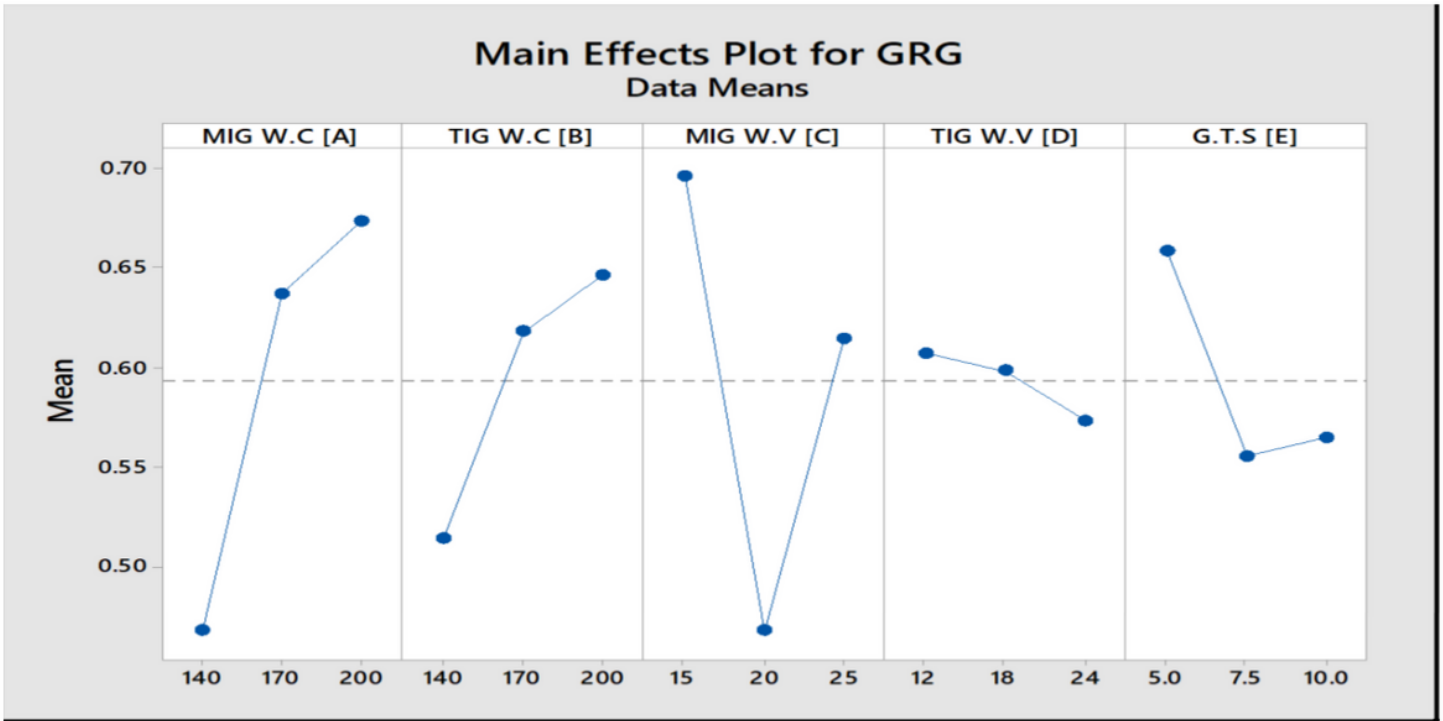


Figure 10

Main effect of plot for GRG

Interaction Plot for GRG Data Means

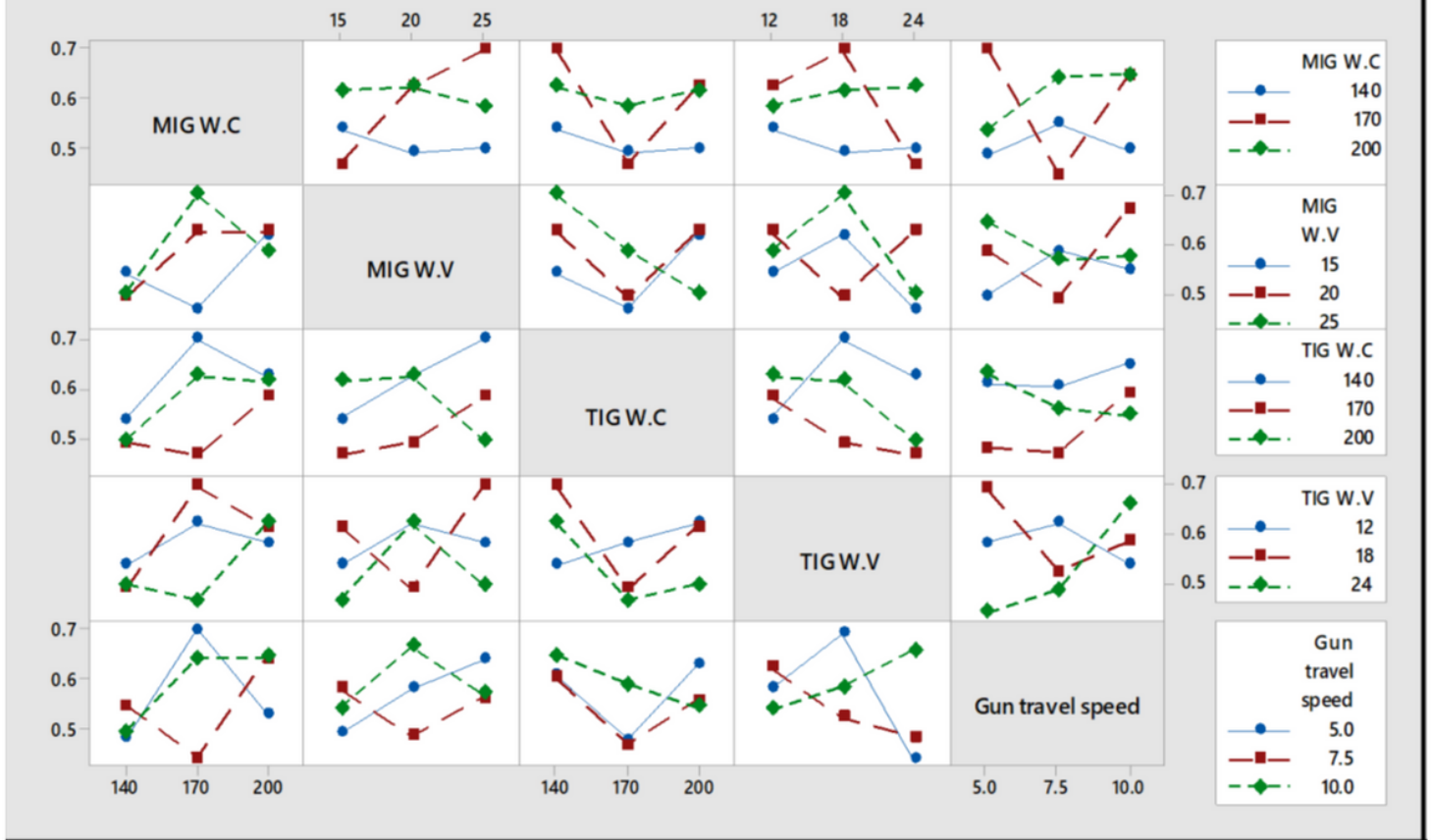


Figure 11

Interaction plot of GRG